Available online at www.sciencedirect.com
ScienceDirect
Vision Research 47 (2007) 776–782
Vision Research
www.elsevier.com/locate/visres

Lack of spontaneous ocular neovascularization and attenuated laser-induced choroidal neovascularization in IGF-I overexpression transgenic mice

Wenzheng Hu [a], Wei Wang [a], Hua Gao [a], Jin Zhong [b], Weiguo Yao [b], Wei-Hua Lee [b], Ping Ye [c], Xiaoxi Qiao [a,*]

[a] Department of Ophthalmology, Indiana University School of Medicine, Indianapolis, IN 46202, USA
[b] Department of Pediatrics, Anatomy and Cell Biology, Indiana University School of Medicine, Indianapolis, IN 46202, USA
[c] Department of Pediatrics, University of North Carolina at Chapel Hill, Chapel Hill, NC, USA

Received 18 August 2006; received in revised form 14 November 2006

Abstract

Robust IGF-I overexpression induces ocular angiogenesis in mice. To investigate the effect of subtle IGF-I overexpression, we examined the ocular phenotype of IGF-II promoter-driven IGF-I transgenic mice. Despite 2.5-fold elevation of IGF-I mRNA in the retina and 29 and 52% increase of IGF-I protein in the retina and aqueous humor, respectively, no ocular abnormality was observed in these transgenics. This was correlated with unaltered VEGF mRNA levels in the transgenic retina. The transgene was also associated with an attenuated laser-induced choroidal neovascularization. Differential expression levels and pattern of IGF-I gene may underlie the different retinal phenotypes in different transgenic lines.
Published by Elsevier Ltd.

Keywords: Insulin-like growth factor I; Transgenic mouse; Choroidal neovascularization

1. Introduction

Neovascular age-related macular degeneration and proliferative diabetic retinopathy, characterized by choroidal neovascularization (CNV) or retinal neovascularization (RNV), are the leading causes of blindness in the developed countries. Due to the limited knowledge of the mechanisms underlies these diseases, current treatments, like laser photocoagulation and anti-angiogenic agents, provide only temporary or partial protection. Much effort has been devoted to determining the pathogenesis of neovascularization and establishing reproducible animal models to assay new treatments.

Insulin-like growth factor (IGF)-I has been associated with the pathological ocular angiogenesis (Burgos et al., 2000; Grant et al., 1993; Lambooij et al., 2003; Smith et al., 1999). There is evidence that IGF-I can act directly as an angiogenic factor on retinal and choriocapillary endothelial cells (Grant, Caballero, & Millard, 1993; Spraul, Baldysiak-Figiel, Lang, & Lang, 2002), and indirectly through the induction of VEGF expression in retinal pigment epithelium (RPE) cells and glial cells (Miele, Rochford, Filippa, Giorgetti-Peraldi, & Van Obberghen, 2000; Punglia et al., 1997; Ruberte et al., 2004; Slomiany & Rosenzweig, 2004a, 2004b). Increased ocular levels of IGF-I in transgenic mice driven by an insulin promoter-I (Insulin/IGF-I transgenic mice) have been reported to result in a condition similar to diabetic retinopathy (Ruberte et al., 2004). A role of IGF-I in vessel formation and remodelling also is suggested by abnormal retinal vascular growth in the IGF-I knockout mice, despite the presence of VEGF (Hellstrom et al., 2001). Furthermore, abundant evidence indicates that IGF-I protects a variety of ocular cells from metabolic and ischemic damage (Bridgewater, Ho, Sauro, & Matsell,

* Corresponding author. Fax: +1 317 274 1288.
E-mail address: xqiao@iupui.edu (X. Qiao).

0042-6989/$ - see front matter Published by Elsevier Ltd.
doi:10.1016/j.visres.2006.11.021

2005; Ozen et al., 2005; Popken et al., 2004; Song et al., 2005; Zhong et al., 2005). IGF-I prevents the degeneration of retinal amacrine cells in culture (Politi, Rotstein, Salvador, Giusto, & Insua, 2001) and R28 retinal precursor cells (Seigel, Chiu, & Paxhia, 2000). In the rat retina, IGF-I protects axotomized retinal ganglion cells from secondary cell death (Kermer, Klocker, Labes, & Bahr, 2000), and prevents cell death under in vitro conditions of hypoxia or serum-starvation (Seigel et al., 2000).

Several lines of IGF-I transgenic mice under different promoters have been generated to date (Ruberte et al., 2004; Ye, Carson, & D'Ercole, 1995a, Ye, Carson, & D'Ercole, 1995b; Ye, Lee, & D'Ercole, 2000; Ye, Xing, Dai, & D'Ercole, 1996). Characterization of these transgenics revealed differential phenotypes in the brain as well as other peripheral organs. However, except diabetes-like retinopathy in the line of Insulin/IGF-I transgenic, the ocular effects of altered IGF-I expression in the other lines are not known. It is not clear whether overexpression of IGF-I in the eye is always associated with ocular pathology. A line of transgenic mice overexpressing IGF-I driven by an IGF-II promoter (IGF-II/IGF-I transgenic mice) is featured with significant transgene expression only in the central nervous system (CNS) with particularly high level in the cerebellum (Ye et al., 1996; Zhong et al., 2005). As retina is part of nervous system and IGF-II is expressed in the retina (Arnold et al., 1993), an increased level of IGF-I is expected in the retina of IGF-II/IGF-I mice. Therefore, in the present study, we characterized the ocular phenotype and examined the expression patterns of IGF-I and VEGF in the retina of the transgenic mice. Potential effects of IGF-I overexpression on the formation of CNV induced by laser photocoagulation (Lambert et al., 2003; Ming et al., 2004; Sakurai, Anand, Ambati, van Rooijen, & Ambati, 2003; Silva et al., 2005; Tobe et al., 1998) were also investigated.

2. Materials and methods

2.1. Animals

Fourteen pairs of adult IGF-II/IGF-I transgenic mice and their age and sex matched wildtype littermates were used in the study. Generation of the IGF-II/IGF-I transgenic mice and determination of the genotype has been described previously (Ye et al., 1996; Zhong et al., 2005). Briefly, these transgenic mice carry a 6.9 kb fusion gene with a 5.7 kb fragment of the 5′ mouse IGF-II genomic regulatory region driving the expression of a human IGF-I cDNA. Mice were subject for PCR genotyping of IGF-I transgene using tail genomic DNA.

All animals were maintained on a 12/12 h (light/dark) cycle at 22 °C, and were provided access to water and diet ad libitum. All procedures were performed with strict adherence to the guidelines for animal care and experimentation prepared by the Association for Research in Vision and Ophthalmology and approved by the Indiana University Animal Care and Use Committee.

2.2. Slit-lamp microscopy, fundus photography and fluorescein angiography

Mice were anesthetized using Avertin 0.02 ml/gm body weight (1.25% w/v tribromoethanol, 0.8% v/v amyl alcohol). Topical 1% tropicamide and 2.5% phenylephrine were administered for pupillary dilation. Before laser photocoagulation and eye enucleation, all mice were examined under slit-lamp microscopy, fundus photography and fluorescein angiography (FA). For FA evaluations, 25% sodium fluorescein (0.1 mg/kg) was administered intraperitoneally. Individual lesion sites, photographed during late phase fluorescein angiography, were subjected to analysis for the presence and intensity of staining and leakage using the murine FA leakage score (0 "no leakage" to 3 "strong leakage") as reported previously (Hu et al., 2005; Takahashi, Kishi, Muraoka, & Shimizu, 1998).

2.3. Laser photocoagulation to induce CNV

Five pairs of IGF-I transgenics and their wildtype littermates received laser photocoagulation at 3 and half months of age. After pupillary dilation, anesthetized animals were positioned before a slit-lamp (Carl Zeiss Meditec, Jena, Germany) laser-delivery system. The fundus was visualized using a cover slip with 2.5% hydroxypropyl methylcellulose solution (Goniosol) as an optical coupling agent. A diode laser (OcuLight GL, Iris Medical Instrument, Inc., Mountain View, CA) was used for photocoagulation (532 nm wavelength, 0.05 s duration, 75 μm spot size and 120 mW power), which most reliably produced acute vapor bubble, suggestive of Bruch's membrane rupture (Hu et al., 2005; Lambert et al., 2003; Tobe et al., 1998). In all experiments, a series of four photocoagulation sites were concentrically placed at equal distances (~75–100 μm) around the optic disk in each eye. Two weeks after laser photocoagulation, when CNV was well established (Tobe et al., 1998) and reached maximum size (Espinosa-Heidmann et al., 2002), eyes were processed for histological analysis.

2.4. Quantitative real-time RT-PCR

Total RNA was isolated from retinal tissues of the left eye in two pairs of IGF-II/IGF-I transgenic mice and their wildtype littermates at 4 months of age, using RNeasy Mini Kit (Qiagen, Valencia, California) following the manufacturer's protocol. Quantitative real-time RT-PCR, after reverse transcription, was performed to determine the gene expression levels of IGF-I and VEGF. Briefly, 1 μg total RNA was used for the first-strand cDNA synthesis (SuperScript II reverse transcriptase; Invitrogen, Carlsbad, CA) with Oligo$(dT)_{12-18}$ primer (Invitrogen) according to the manufacturer's instructions. Real-time PCR was performed in triplicate using 25 μl of reaction mixture containing primer, cDNA, and iQ SYBR Green Supermix (Bio-Rad, Hercules, CA) on a single-color real-time PCR detection system (MyiQ; Bio-Rad). Reactions were started with denaturing at 94 °C for 5 min and followed by 40 cycles of denaturing at 94 °C for 30 s, annealing and extending at 60 °C for 45 s. Glyceraldehyde-3-phosphate dehydrogenase (GAPDH) was used as the reference gene, and relative levels of IGF-I and VEGF compared with that of GAPDH were calculated.

The sequences of specific primers are listed as follows. Mouse GAPDH: 5′-TCC TGG TAT GAC AAT GAA TAC GGC-3′ (forward) and 5′-TCT TGC TCA GTG TCC TTG CTG G-3′ (reverse). Mouse IGF-I: 5′-TTC ACA TCT CTT CTA CCT GGC-3′ (forward) and 5′-TCT TGT TTC CTG CAC TTC CT-3′ (reverse). Transgene (human IGF-I): 5′-GGA CCG GAG ACG CTC TGC GG-3′ (forward) and 5′-CTG CGG TGG CAT GTC ACT CT-3′ (reverse). Mouse VEGF: 5′-AGG CTG CAC CCA CGA CAG AA-3′ (forward) and 5′-CTT TGG TCT GCA TTC ACA TC-3′ (reverse).

2.5. In situ hybridization

Right eyes of six pairs of mice at 2, 4 and 10 months of age were fixed in 4% phosphate-buffered paraformaldehyde solution overnight at 4 °C. Tissues were dehydrated, embedded in paraffin, serially sectioned (6 μm). Standard protocols of riboprobe in situ hybridization were followed as described in detail previously (Gao, Qiao, Hefti, Hollyfield, & Knusel, 1997; Qiao, Hefti, Knusel, & Noebels, 1996). A human IGF-I cDNA clone consisting of 369 bp coding region and a 570 bp mouse VEGF cDNA clone in pBluescript SK plasmid obtained as a generous gift

from Dr. Salman Hyder at the University of Texas in Houston (Hyder, Nawaz, Chiappetta, & Stancel, 2000) were used to generate riboprobes. ^{35}S-labeled riboprobes were transcribed using Riboprobe Gemini System according to manufacturer's instructions (Promega Inc., Madison, WI). The tissue sections were deparaffinized in xylene followed by rehydration. The sections were pretreated with 10 mg/ml proteinase K at 37 °C for 20 min, and then 0.25% acetic anhydrite in 0.1 M triethanolamide for 10 min. The sections were incubated at 50 °C on a slide warmer overnight with a probe solution containing 5×10^6 cpm/ml ^{35}S-labeled probes, 50% formamide, 10% dextran sulfate, 300 mM NaCl, 0.5 mg/ml tRNA, 10 mM DTT, 0.02% Ficoll, 0.02% polyvinyl-pyrolidone, 0.02% BSA and 1 mM EDTA in 10 mM Tris–HCl (pH 8.0). Following hybridization, the slides were rinsed in 4× SSC (150 mM NaCl and 15 mM sodium citrate), digested with 20 μg/ml RNase A at 37 °C for 30 min, washed through descending concentrations of SSC to 0.1× SSC at 60–70 °C. The slides were then dehydrated, dried and coated with NTB-2 emulsion (Kodak Inc., Rochester, NY). Following exposure in the dark for 4 weeks, the emulsion was developed and sections were counter-stained with hematoxylin.

2.6. Radioimmunoassay of IGF-I

Retinal tissues of six pairs of eyes were homogenized in ice cold lysis buffer containing 1% Nonidet P-40, 0.1% sodium dodecyl sulfate (SDS), 1 mM PMSF, 1 mM Na_3VO_4, 1 mM NaF, 1 μg/ml aprotinin, 1 μg/ml leupeptin, 1 μg/ml pepstatin and 50 mM Tris–HCl, pH 7.4. The suspension was centrifuged at 10,000 rpm for 30 min at 4 °C and the supernatant was removed for protein concentration measurement by a Bio-Rad protein assay kit. Total IGF-I concentrations in the retina and in aqueous humor were determined by radioimmunoassay (RIA) (ALPCO Diagnostics, Windham, NH) using the standard procedure suggested by the manufacturer, in which special sample preparation is not required before measurement. The sensitivity of the assay is 0.02 ng/ml. The concentration in the retina was expressed as ng/mg total protein.

2.7. Histology and CNV assessment

Serial, radial tissue sections through each recovered lesion site were evaluated in their entirety to quantify the extent of fibrovascular proliferation. For statistical analyses, maximum CNV membrane thickness measurement, which typically occurred at or near the center of the initial trauma site, were obtained from digital photographs (Nikon CoolPix 990 modified camera system) and then were converted to μm measurements (using graticule image measurements for comparison). As reported previously (Ciulla et al., 2003), this technique demonstrated reproducibility of measurements within ±2 μm using a random sampling of representative masked lesions. CNV membrane mean thickness values for each group were obtained using the maximum thickness measurements of each of the four lesion sites per eye to then determine an average value for each site within IGF-I transgenic mice and from wildtype mice. The values were expressed as means ± standard deviation (SD).

2.8. Statistical analysis

The Student's *t*-test was used to compare the differences of CNV membrane mean thickness and FA leakage mean score between the transgenic and wildtype groups. *p* values of less than 0.05 were considered to be significant.

3. Results

3.1. No spontaneous ocular neovascularization in the IGF-I transgenic mice

Slit-lamp microscopy revealed no evidence of cornea or iris neovascularization or of cataracts in the IGF-II/IGF-I transgenic mice at any age up to 10 months. On funduscopic examination no retinal hemorrhage or vessel dilatation was noticed. Fluorescein angiography did not reveal any leakage before laser photocoagulation, suggesting that no spontaneous RNV or CNV occurred. Histologically, no abnormality of ocular morphology was noticed and no spontaneous retinal/choroidal neovascularization was observed at ages up to 10 months (image not presented).

3.2. Significant overexpression of IGF-I mRNA in the transgenic retina

To confirm that IGF-I is overexpressed in the retina, the levels of IGF-I mRNA were measured by both real-time RT-PCR and in situ hybridization. As shown in Fig. 1, the levels of endogenous mouse IGF-I mRNA between the transgenic and wildtype groups were not significantly different ($p > 0.05$). Significant expression of the human IGF-I transgene was detected in the transgenic but not in the wildtype retina. As the amplification efficiency in two sets of reactions may not be exactly same, we can only estimate the total amount of IGF-I mRNA after standardized with the internal control molecule GAPDH. The sum of the IGF-I mRNA ratio in the transgenic retina, including transgenic and endogenous IGF-I, was 2.5-fold of that in the wildtype. In situ hybridization demonstrated that the increased signals of IGF-I mRNA in the transgenics were predominantly concentrated in the ganglion cell layer and inner segment of photoreceptors (Fig. 2). This overexpression was evident at all ages studied (2, 4 and 10 months of age).

3.3. No upregulation of VEGF mRNA in the transgenic retina

Because IGF-I has been suggested to mediate pathological angiogenesis through induction of VEGF expression in

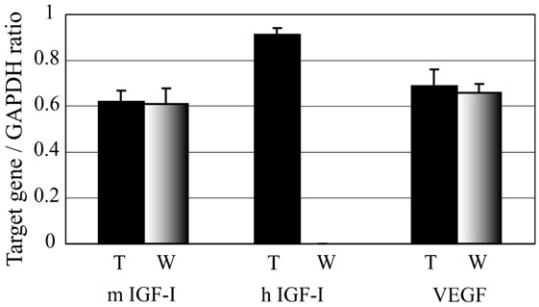

Fig. 1. Quantitative real-time RT-PCR of IGF-I and VEGF mRNAs in the retina of IGF-II/IGF-I transgenic (T) and wildtype (W) mice at 4 months of age. The endogenous mouse IGF-I (mIGF-I) level was not significantly altered in the transgenic mice comparing to that in the wildtype. High levels of human IGF-I transgene (hIGF-I) were detected in the transgenic but not in the wildtype retina. The sum of the ratio of total IGF-I over GAPDH signals, including transgenic and endogenous IGF-I, in the transgenic retina was 2.5-fold of that in the wildtype. There was no significant difference in the VEGF/GAPDH ratio between the transgenic and the wildtype mice.

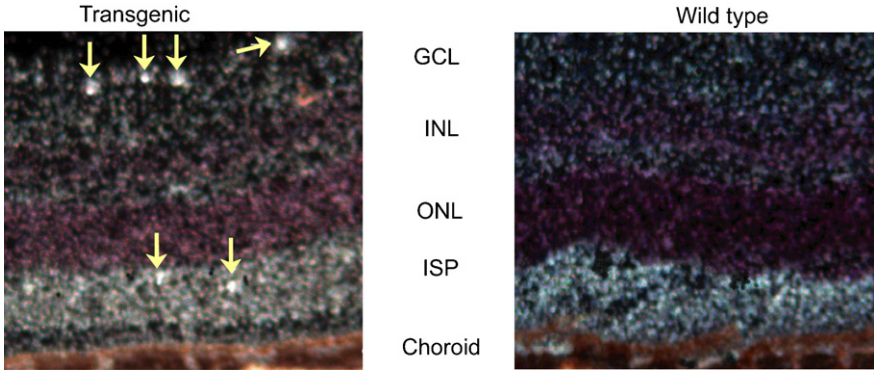

Fig. 2. In situ hybridization of the expression pattern of IGF-I mRNA in the adult IGF-II/IGF-I transgenic and wildtype mice. IGF-I mRNA was increased in the transgenic retina at 2, 4 and 10 months of age (images showed at 4 months of age). The increased signals, shown as bright clusters (pointed by arrows in the left panel) in the dark-field images, were located mainly in the ganglion cell layer and inner segment of photoreceptor. GCL, ganglion cell layer; INL, inner nuclear layer; ONL, outer nuclear layer; ISP, inner segment of photoreceptor.

the Insulin/IGF-I transgenic mice, VEGF mRNA level was assessed by real-time RT-PCR and in situ hybridization in the retina of IGF-II/IGF-I transgenic mice. Real-time RT-PCR revealed similar levels of VEGF mRNA in the retina of transgenic and wildtype at 4 months of age without statistic difference ($p > 0.05$). The pattern of VEGF mRNA in the transgenic retina mapped by in situ hybridization was also not different from that in the wildtype (image not presented). The results are consistent with lack of spontaneous angiogenesis in the retina of this mutant line.

3.4. Moderate increase of IGF-I concentration in the transgenic retina and aqueous humor

The expression of IGF-I protein was confirmed by radioimmunoassay. As shown in Fig. 3, the IGF-I concentration had an increase of 29% in the transgenic retina (4.61 ± 0.35 ng/mg total protein) when compared to that in the wildtype (3.57 ± 0.11 ng/mg total protein). The increase of IGF-I protein level was even higher in the transgenic aqueous humor (9.44 ± 0.33 ng/ml) 52% more than that in the wildtype (6.20 ± 1.87 ng/ml).

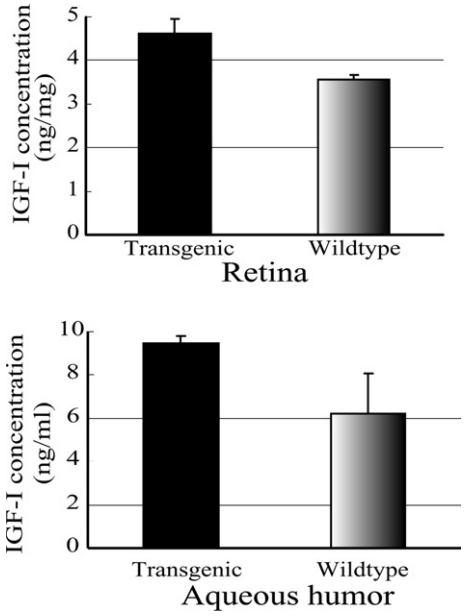

Fig. 3. Radioimmunoassay of IGF-I levels in the retina and aqueous humor at 4 months of age. Compared to the wildtype, IGF-I concentration has an increase of 29% in the transgenic retina and 52% in the transgenic aqueous humor (six pairs of eyes).

3.5. Less CNV membranes induced in the transgenic mice

To determine if overexpression of IGF-I may facilitate lesion-trigged angiogenic response, laser photocoagulation model was used to induce choroidal neovascularization. FA examination 2 weeks after the laser treatment revealed less subretinal fluorescein leakage at the laser sites in the transgenic mice than that in the wildtype (Fig. 4). Quantitative analysis of fluorescein leakage was statistically significant with lower FA score at the lesion sites in the transgenic mice (mean FA score of 1.8 ± 0.8) than that in the wildtype mice (mean score 2.2 ± 0.8; $p < 0.05$).

Histologically, the CNV membrane was well established in 2 weeks after laser photocoagulation. The dome-shaped CNV membrane contained fibrovascular tissue with vessels, scattered RPE cells, and macrophage-like cells. Morphologic features of CNV membranes in the transgenic mice were comparable to those in the wildtype mice (Fig. 5). Quantitative histopathologic analysis demonstrated that the mean CNV membrane thickness of 40 laser sites was significantly thinner in the transgenic (48.9 ± 17.8 μm) than that in the wildtype (62.7 ± 22.9 μm; $p = 0.01$). The results indicate an attenuated, rather than intensified lesion-induced angiogenic response in the IGF-II/IGF-I transgenic mice, which does not support any facilitative role of IGF-I in this model of CNV pathogenesis.

4. Discussion

In this line of IGF-I transgenic mice, the overexpression of IGF-I is localized predominantly to the retinal ganglion

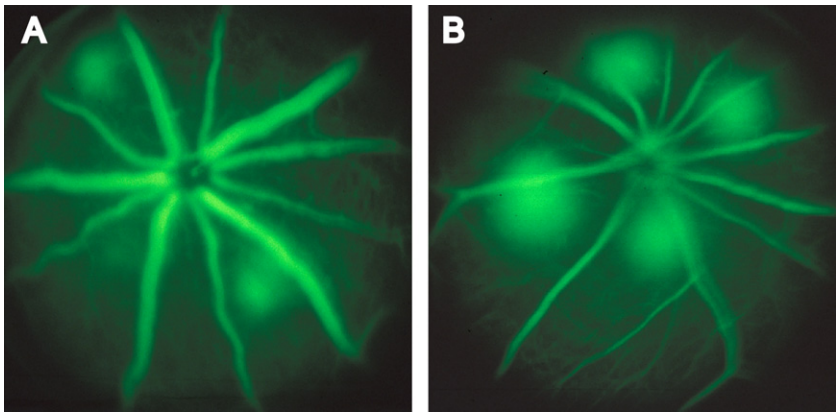

Fig. 4. Fluorescein angiography at 2 weeks after laser photocoagulation in the retina of transgenic (A) and wildtype (B) mice. The transgenics had less fluorescein leakage with a mean score of 1.8, versus 2.2 in the wildtype mice (40 laser sites of each group). (A) Scored as 0, 2, 1, 2 from 1 o'clock to 12 o'clock. (B) Scored as 3, 3, 3, 3.

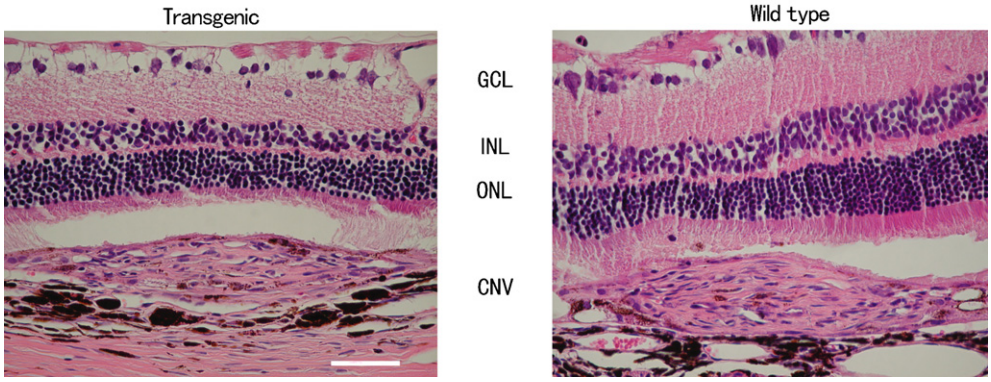

Fig. 5. Choroidal neovascular membranes developed in the IGF-II/IGF-I transgenic mice and their wildtype littermates in 2 weeks after laser photocoagulation. The membrane was morphologically comparable in both groups. The thickness of choroidal neovascular membrane showed above was 50 μm (transgenic) and 57 μm (wildtype). The mean thickness of membranes was 22% thinner in the transgenic mice than that in the wildtype mice (40 laser sites in each group). Scale bar: 50 μm. GCL, ganglion cell layer; INL, inner nuclear layer; ONL, outer nuclear layer.

cell layer and inner segment of photoreceptors. Despite the significant elevation of IGF-I mRNA levels in the eyes of transgenic mice, no spontaneous neovascularization in cornea, iris, retina or choroid was observed up to 10 months of age. These results are different from the Insulin/IGF-I transgenic mouse reported by Ruberte et al. (2004), in which the increased ocular levels of IGF-I lead to diabetes-like eye disease.

Several possibilities may explain the differences between these two lines of IGF-I transgenic mice. Different promoters drive these transgenes and lead to different sites of IGF-I overexpression in the retina. In IGF-II/IGF-I transgenic mice, IGF-I mRNA is predominantly overexpressed at ganglion cell layer and inner segment of photoreceptor, while the Insulin/IGF-I transgenic mice, IGF-I is expressed in the outer plexiform layer and in the inner segment of photoreceptors. The different locations of the IGF-I overexpression could influence the local availability of IGF-I, and result in different phenotypes. Another explanation is the magnitude of IGF-I overexpression in the two transgenic lines. IGF-II/IGF-I transgenic mice only showed moderate overexpression of IGF-I in the retina and aqueous humor, while in the Insulin/IGF-I transgenic mice, the levels of IGF-I in the retina and aqueous humor were ten to a 100-folds higher than those in the wildtype mice. Danis et al. reported that different intravitreous IGF-I levels induced different ocular changes, with larger doses producing a retinal microangiopathy, while lower doses showed fewer clinical and histopathologic changes (Danis & Bingaman, 1997). It is highly possible that different ocular IGF-I expression levels may dictate the extent of ocular changes. Finally, there was no significant upregulation of VEGF observed in the IGF-II/IGF-I transgenic retina, while a 2-fold increase of VEGF transcripts was detected in the Insulin/IGF-I transgenic eyes. This could be the most important and most direct cause for the different ocular phenotypes between the two transgenic lines.

Interestingly, our data clearly showed that the IGF-II/IGF-I transgenic mice developed less CNV membranes and fluorescein leakage following laser treatment than their wildtype littermates. IGF-I has well documented anti-apoptotic actions on many cell types (Bridgewater et al., 2005; Ozen et al., 2005; Popken et al., 2004; Song et al., 2005; Zhong et al., 2005), including retinal precursor cells,

ganglion cells and amacrine cells. It is possible that less cell apoptosis after laser-trauma attenuated the formation of CNV. In addition, IGF-I bioactivity is influence by many factor, such as the presence of IGF binding proteins (IGFBPs) and the magnitude of IGF receptor expression (Clemmons, 1998; Delafontaine, Song, & Li, 2004), which is responsible for mediating most of IGF-I action. It has been reported that granule neurons in the cerebellum of IGF-II/IGF-I transgenic mice express high levels of IGF binding protein 5, which has the capacity to block some IGF-I activities (Zhong et al., 2005). It is possible, therefore, IGFBPs affect IGF-I bioactivities and alter the overall outcome in any specific cellular location. Additional experiments are necessary to determine the underlying mechanisms for the attenuated response of laser-induced CNV in this transgenic mouse model.

Acknowledgment

Supported by Reeve's Foundation and Research to Prevent Blindness Foundation.

References

Arnold, D. R., Moshayedi, P., Schoen, T. J., Jones, B. E., Chader, G. J., & Waldbillig, R. J. (1993). Distribution of IGF-I and -II, IGF binding proteins (IGFBPs) and IGFBP mRNA in ocular fluids and tissues: potential sites of synthesis of IGFBPs in aqueous and vitreous. *Experimental Eye Research, 56*(5), 555–565.

Bridgewater, D. J., Ho, J., Sauro, V., & Matsell, D. G. (2005). Insulin-like growth factors inhibit podocyte apoptosis through the PI3 kinase pathway. *Kidney International, 67*(4), 1308–1314.

Burgos, R., Mateo, C., Canton, A., Hernandez, C., Mesa, J., & Simo, R. (2000). Vitreous levels of IGF-I, IGF binding protein 1, and IGF binding protein 3 in proliferative diabetic retinopathy: a case-control study. *Diabetes Care, 23*(1), 80–83.

Ciulla, T. A., Criswell, M. H., Danis, R. P., Fronheiser, M., Yuan, P., Cox, T. A., et al. (2003). Choroidal neovascular membrane inhibition in a laser treated rat model with intraocular sustained release triamcinolone acetonide microimplants. *British Journal of Ophthalmology, 87*(8), 1032–1037.

Clemmons, D. R. (1998). Role of insulin-like growth factor binding proteins in controlling IGF actions. *Molecular and Cellular Endocrinology, 140*(1–2), 19–24.

Danis, R. P., & Bingaman, D. P. (1997). Insulin-like growth factor-1 retinal microangiopathy in the pig eye. *Ophthalmology, 104*(10), 1661–1669.

Delafontaine, P., Song, Y. H., & Li, Y. (2004). Expression, regulation, and function of IGF-I, IGF-IR, and IGF-I binding proteins in blood vessels. *Arteriosclerosis, Thrombosis, and Vascular Biology, 24*(3), 435–444.

Espinosa-Heidmann, D. G., Suner, I., Hernandez, E. P., Frazier, W. D., Csaky, K. G., & Cousins, S. W. (2002). Age as an independent risk factor for severity of experimental choroidal neovascularization. *Investigative Ophthalmology and Visual Science, 43*(5), 1567–1573.

Gao, H., Qiao, X., Hefti, F., Hollyfield, J. G., & Knusel, B. (1997). Elevated mRNA expression of brain-derived neurotrophic factor in retinal ganglion cell layer after optic nerve injury. *Investigative Ophthalmology and Visual Science, 38*(9), 1840–1847.

Grant, M. B., Caballero, S., & Millard, W. J. (1993). Inhibition of IGF-I and b-FGF stimulated growth of human retinal endothelial cells by the somatostatin analogue, octreotide: a potential treatment for ocular neovascularization. *Regulatory Peptides, 48*(1–2), 267–278.

Grant, M. B., Mames, R. N., Fitzgerald, C., Ellis, E. A., Aboufriekha, M., & Guy, J. (1993). Insulin-like growth factor I acts as an angiogenic agent in rabbit cornea and retina: comparative studies with basic fibroblast growth factor. *Diabetologia, 36*(4), 282–291.

Hellstrom, A., Perruzzi, C., Ju, M., Engstrom, E., Hard, A. L., Liu, J. L., et al. (2001). Low IGF-I suppresses VEGF-survival signaling in retinal endothelial cells: direct correlation with clinical retinopathy of prematurity. *Proceedings of the National Academy of Sciences of the United States of America, 98*(10), 5804–5808.

Hu, W., Criswell, M. H., Ottlecz, A., Cornell, T. L., Danis, R. P., Lambrou, G. N., et al. (2005). Oral administration of lumiracoxib reduces choroidal neovascular membrane development in the rat laser-trauma model. *Retina, 25*(8), 1054–1064.

Hyder, S. M., Nawaz, Z., Chiappetta, C., & Stancel, G. M. (2000). Identification of functional estrogen response elements in the gene coding for the potent angiogenic factor vascular endothelial growth factor. *Cancer Research, 60*(12), 3183–3190.

Kermer, P., Klocker, N., Labes, M., & Bahr, M. (2000). Insulin-like growth factor-I protects axotomized rat retinal ganglion cells from secondary death via PI3-K-dependent Akt phosphorylation and inhibition of caspase-3 in vivo. *Journal of Neuroscience, 20*(2), 2–8.

Lambert, V., Wielockx, B., Munaut, C., Galopin, C., Jost, M., Itoh, T., et al. (2003). MMP-2 and MMP-9 synergize in promoting choroidal neovascularization. *The FASEB Journal, 17*(15), 2290–2292.

Lambooij, A. C., VanWely, K. H., Lindenbergh-Kortleve, D. J., Kuijpers, R. W., Kliffen, M., & Mooy, C. M. (2003). Insulin-like growth factor-I and its receptor in neovascular age-related macular degeneration. *Investigative Ophthalmology and Visual Science, 44*(5), 2192–2198.

Miele, C., Rochford, J. J., Filippa, N., Giorgetti-Peraldi, S., & Van Obberghen, E. (2000). Insulin and insulin-like growth factor-I induce vascular endothelial growth factor mRNA expression via different signaling pathways. *Journal of Biological Chemistry, 275*(28), 21695–21702.

Ming, Y., Algvere, P. V., Odergren, A., Berglin, L., van der Ploeg, I., Seregard, S., et al. (2004). Subthreshold transpupillary thermotherapy reduces experimental choroidal neovascularization in the mouse without collateral damage to the neural retina. *Investigative Ophthalmology and Visual Science, 45*(6), 1969–1974.

Ozen, S., Akisu, M., Baka, M., Yalaz, M., Sozmen, E. Y., Berdeli, A., et al. (2005). Insulin-like growth factor attenuates apoptosis and mucosal damage in hypoxia/reoxygenation-induced intestinal injury. *Biology of the Neuonate, 87*(2), 91–96.

Politi, L. E., Rotstein, N. P., Salvador, G., Giusto, N. M., & Insua, M. F. (2001). Insulin-like growth factor-I is a potential trophic factor for amacrine cells. *Journal of Neurochemistry, 76*(4), 1199–1211.

Popken, G. J., Hodge, R. D., Ye, P., Zhang, J., Ng, W., O'Kusky, J. R., et al. (2004). In vivo effects of insulin-like growth factor-I (IGF-I) on prenatal and early postnatal development of the central nervous system. *European Journal of Neuroscience, 19*(8), 2056–2068.

Punglia, R. S., Lu, M., Hsu, J., Kuroki, M., Tolentino, M. J., Keough, K., et al. (1997). Regulation of vascular endothelial growth factor expression by insulin-like growth factor I. *Diabetes, 46*(10), 1619–1626.

Qiao, X., Hefti, F., Knusel, B., & Noebels, J. L. (1996). Selective failure of brain-derived neurotrophic factor mRNA expression in the cerebellum of stargazer, a mutant mouse with ataxia. *Journal of Neuroscience, 16*(2), 640–648.

Ruberte, J., Ayuso, E., Navarro, M., Carretero, A., Nacher, V., Haurigot, V., et al. (2004). Increased ocular levels of IGF-I in transgenic mice lead to diabetes-like eye disease. *The Journal of Clinical Investigation, 113*(8), 1149–1157.

Sakurai, E., Anand, A., Ambati, B. K., van Rooijen, N., & Ambati, J. (2003). Macrophage depletion inhibits experimental choroidal neovascularization. *Investigative Ophthalmology and Visual Science, 44*(8), 3578–3585.

Seigel, G. M., Chiu, L., & Paxhia, A. (2000). Inhibition of neuroretinal cell death by insulin-like growth factor-1 and its analogs. *Molecular Vision, 6*, 157–163.

Silva, R. L., Saishin, Y., Saishin, Y., Akiyama, H., Kachi, S., Aslam, S., et al. (2005). Suppression and regression of choroidal neovascularization by polyamine analogues. *Investigative Ophthalmology and Visual Science, 46*(9), 3323–3330.

Slomiany, M. G., & Rosenzweig, S. A. (2004a). Autocrine effects of IGF-I-induced VEGF and IGFBP-3 secretion in retinal pigment epithelial cell line ARPE-19. *American Journal of Physiology Cell Physiology, 287*(3), C746–C753.

Slomiany, M. G., & Rosenzweig, S. A. (2004b). IGF-I-induced VEGF and IGFBP-3 secretion correlates with increased HIF-1 alpha expression and activity in retinal pigment epithelial cell line D407. *Investigative Ophthalmology and Visual Science, 45*(8), 2838–2847.

Smith, L. E., Shen, W., Perruzzi, C., Soker, S., Kinose, F., Xu, X., et al. (1999). Regulation of vascular endothelial growth factor-dependent retinal neovascularization by insulin-like growth factor-1 receptor. *Nature Medicine, 5*(12), 1390–1395.

Song, Y. H., Li, Y., Du, J., Mitch, W. E., Rosenthal, N., & Delafontaine, P. (2005). Muscle-specific expression of IGF-I blocks angiotensin II-induced skeletal muscle wasting. *Journal of Clinical Investigation, 115*(2), 451–458.

Spraul, C. W., Baldysiak-Figiel, A., Lang, G. K., & Lang, G. E. (2002). Octreotide inhibits growth factor-induced bovine choriocapillary endothelial cells in vitro. *Graefes Archive for Clinical and Experimental Ophthalmology, 240*(3), 227–231.

Takahashi, K., Kishi, S., Muraoka, K., & Shimizu, K. (1998). Reperfusion of occluded capillary beds in diabetic retinopathy. *American Journal of Ophthalmology, 126*(6), 791–797.

Tobe, T., Ortega, S., Luna, J. D., Ozaki, H., Okamoto, N., Derevjanik, N. L., et al. (1998). Targeted disruption of the FGF2 gene does not prevent choroidal neovascularization in a murine model. *American Journal of Pathology, 153*(5), 1641–1646.

Ye, P., Carson, J., & D'Ercole, A. J. (1995a). In vivo actions of insulin-like growth factor-I (IGF-I) on brain myelination: studies of IGF-I and IGF binding protein-1 (IGFBP-1) transgenic mice. *Journal of Neuroscience, 15*(11), 7344–7356.

Ye, P., Carson, J., & D'Ercole, A. J. (1995b). Insulin-like growth factor-I influences the initiation of myelination: studies of the anterior commissure of transgenic mice. *Neuroscience Letter, 201*(3), 235–238.

Ye, P., Lee, K. H., & D'Ercole, A. J. (2000). Insulin-like growth factor-I (IGF-I) protects myelination from undernutritional insult: studies of transgenic mice overexpressing IGF-I in brain. *Journal of Neuroscience Research, 62*(5), 700–708.

Ye, P., Xing, Y., Dai, Z., & D'Ercole, A. J. (1996). In vivo actions of insulin-like growth factor-I (IGF-I) on cerebellum development in transgenic mice: evidence that IGF-I increases proliferation of granule cell progenitors. *Brain Research Developmental Brain Research, 95*(1), 44–54.

Zhong, J., Deng, J., Phan, J., Dlouhy, S., Wu, H., Yao, W., et al. (2005). Insulin-like growth factor-I protects granule neurons from apoptosis and improves ataxia in weaver mice. *Journal of Neuroscience Research, 80*(4), 481–490.